Journal of Organometallic Chemistry, 478 (1994) 153–160

An analysis of the metal–metal bonding in organodirhenium complexes containing Re–Re double bonds

Timothy A. Barckholtz, Bruce E. Bursten

Department of Chemistry, The Ohio State University, Columbus, OH 43210 (USA)

Gerald P. Niccolai and Charles P. Casey

Department of Chemistry, University of Wisconsin, Madison, WI 53706 (USA)

(Received November 5, 1993)

Abstract

Fenske–Hall molecular orbital calculations are used to describe the Re–Re bonding in the low-valent d^6–d^6 dimer $[CpRe(CO)_2]_2$ (**1**) and the high-valent d^2–d^2 dimer $[HCRe(OH)_2]_2$ (**2**), which are models for recently synthesized compounds. Both **1** and **2** contain Re–Re double bonds, corresponding to diamagnetic $\sigma^2\pi^4\delta^2\delta^{*2}\pi^{*2}$ and $\sigma^2\pi^2$ metal–metal bonding configurations, respectively. The bonding in the hypothetical low-valent/high-valent complex $[CpRe(CO)_2][Re(CH)(OH)_2]$ is also discussed.

Key words: Molecular orbital calculations; Rhenium; Carbonyl; Hydroxide; Heterobimetallics; Metal–metal bonding

1. Introduction

Two of the most active research areas in inorganic chemistry are organometallics and metal–metal multiple bonding. Hence, it is not surprising that the intersection of these two fields, the chemistry of dinuclear organometallics with metal–metal multiple bonds, has been extensively developed in recent years [1]. Until recently, all organometallics containing metal–metal double bonds also possessed supporting ligands that bridged the metal–metal bond [2]. Thus, it is quite remarkable that within the space of one year two very different compounds have been synthesized containing rhenium–rhenium double bonds unsupported by fully bridging ligands; Casey and coworkers synthesized the d^6–d^6 dimer $[Cp^*Re(CO)_2]_2$ (**1***, $Cp^* = C_5Me_5$) [3], which contains two semibridging carbonyl ligands, while Schrock and coworkers prepared the d^2–d^2 complex $[RCRe(OR)_2]_2$ (**2′**, $R = {}^tBu$) [4], which contains no bridging ligands.

We have previously used molecular orbital calculations to analyze the bonding in a multitude of dinuclear organometallic complexes, with emphasis on both metal–metal and metal–ligand interactions [5]. We have also been interested in comparing the electronic structures of low-valent and high-valent organometallic

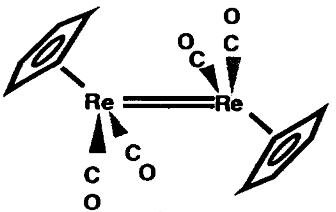

1

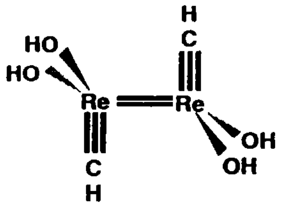

2

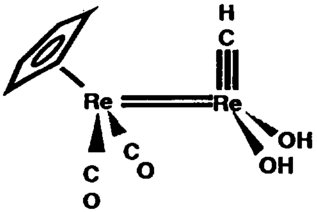

3

Correspondence to: Professor B.E. Bursten.

SSDI 0022-328X(94)24447-Q

Elsevier Science S.A.

fragments, including the potential for metal–metal bonding between them [5–7]. In this contribution, we focus on the metal–metal multiple bonding in model complexes of **1*** and **2′**. In order to do so, we have carried out molecular orbital calculations on $[CpRe(CO)_2]_2$ (**1**, $Cp = C_5H_5$) and $[HCRe(OH)_2]_2$ (**2**). We also explore the possibility of Re–Re bonding in the hypothetical mixed low-valent/high-valent dinuclear complex $[CpRe(CO)_2][Re(CH)(OH)_2]$ (**3**).

2. Results and discussion

2.1. $CpRe(CO)_2$ and $HCRe(OH)_2$

In order to discuss the Re–Re bonding in **1**, **2** and **3**, it is instructive to review first the frontier orbitals of the mononuclear fragments $CpRe(CO)_2$ (**4**) and $HCRe(OH)_2$ (**5**). We have performed calculations on both **4** and **5**, in geometries based on mononuclear 'halves' of **1** and **2**.

The electronic structure of 16e d^6 $CpML_2$ fragments has been discussed previously by several researchers. Hofmann investigated the electronic structure of $CpMn(CO)_2$ in a pyramidal geometry such as the one used here (*i.e.*, as a three-legged piano stool with a missing leg) [8]. Lichtenberger *et al.* have studied $CpMn(CO)_2$ and examined the bonding capabilities of its frontier orbitals [9,10]. As part of their study, they viewed the dimerization of $CpMn(CO)_2$, albeit at long Mn–Mn distances taken from the structure of $[CpMn(CO)_2]_2(\mu\text{-}CH_2)$ [11].

In an approach similar to those taken in the above studies, we view the electronic structure of **4** as derived from the removal of a CO ligand from $CpRe(CO)_3$ (**6**). The resulting picture is depicted as the left-hand side of Fig. 1. Theoretical and experimental studies of **6** confirm the presence of three 'pseudo-t_{2g}' dπ orbitals which are involved in extensive π-back-bonding to the CO ligands [12]. The other two metal d orbitals comprise a set of 'pseudo-e_g' orbitals which are destabilized by metal–ligand σ interactions. Thus, the familiar 'three below two' pattern of predominantly metal d orbitals emerges, consistent with the isolobality of d^6 $CpML_3$ and d^6 ML_6 complexes.

Removal of one of the CO ligands of **6** has two major effects with respect to potential metal–metal bond formation. First, the dσ orbital used as an accep-

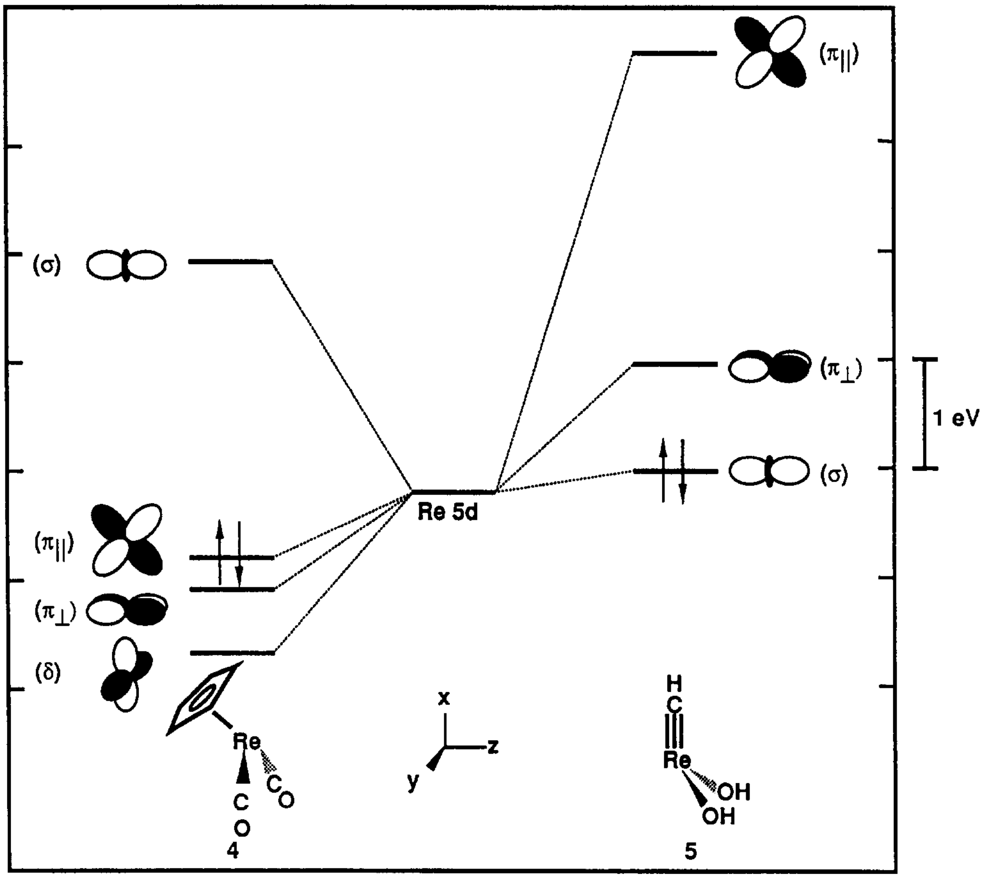

Fig. 1. Valence orbitals for the fragments $CpRe(CO)_2$ (**4**, left) and $HCRe(OH)_2$ (**5**, right). Only the 5d orbital contributions of Re are shown.

tor orbital for the CO is substantially lowered in energy. Second, the dπ orbitals rehybridize in such a way that one of them is directed in an appropriate fashion to foster the formation of a metal–metal π bond. The symmetry properties of the valence orbitals of **4** with respect to Re–Re bond formation are also given in Fig. 1. The fragment contains one orbital of σ and one of δ symmetry, along with two orbitals of π symmetry. The two π orbitals have different symmetry with respect to the mirror plane of the fragment; one lies in the plane containing the Cp centroid ($\pi_{\|}$) while one lies in the plane perpendicular to it ($\pi_{\perp}$).

As with **4**, the orbital energetics for the high-valent fragment **5** can be derived from a stable molecule, albeit a little more indirectly. As shown in eqn. (1), the removal of an alkoxide anion from the d^0 complex (RC)W(OR$'$)$_3$ [13] (**7**) gives a fragment (**7a**) that is isolobal to d^2 **5**, although with two fewer electrons.

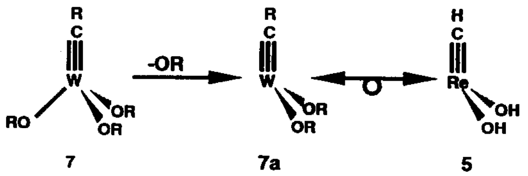

(1)

The valence orbitals of **5** are shown on the right-hand side of Fig. 1. Three of the 5d orbitals of Re are strongly destabilized by the formation of the Re–C triple bond, as is typical for alkylidyne complexes [14,15]. If the Re–C axis is used for quantization, these orbitals have σ, π and π symmetry. The most destabilized of these also has π symmetry with respect to Re–Re bond formation, and is labeled $\pi_{\|}$ in Fig. 1. The two d orbitals that have δ symmetry with respect to the Re–C bond are appropriately oriented to form the Re–Re σ and π bonds; these orbitals, which are slightly perturbed by admixture of Re 6s and by inter-

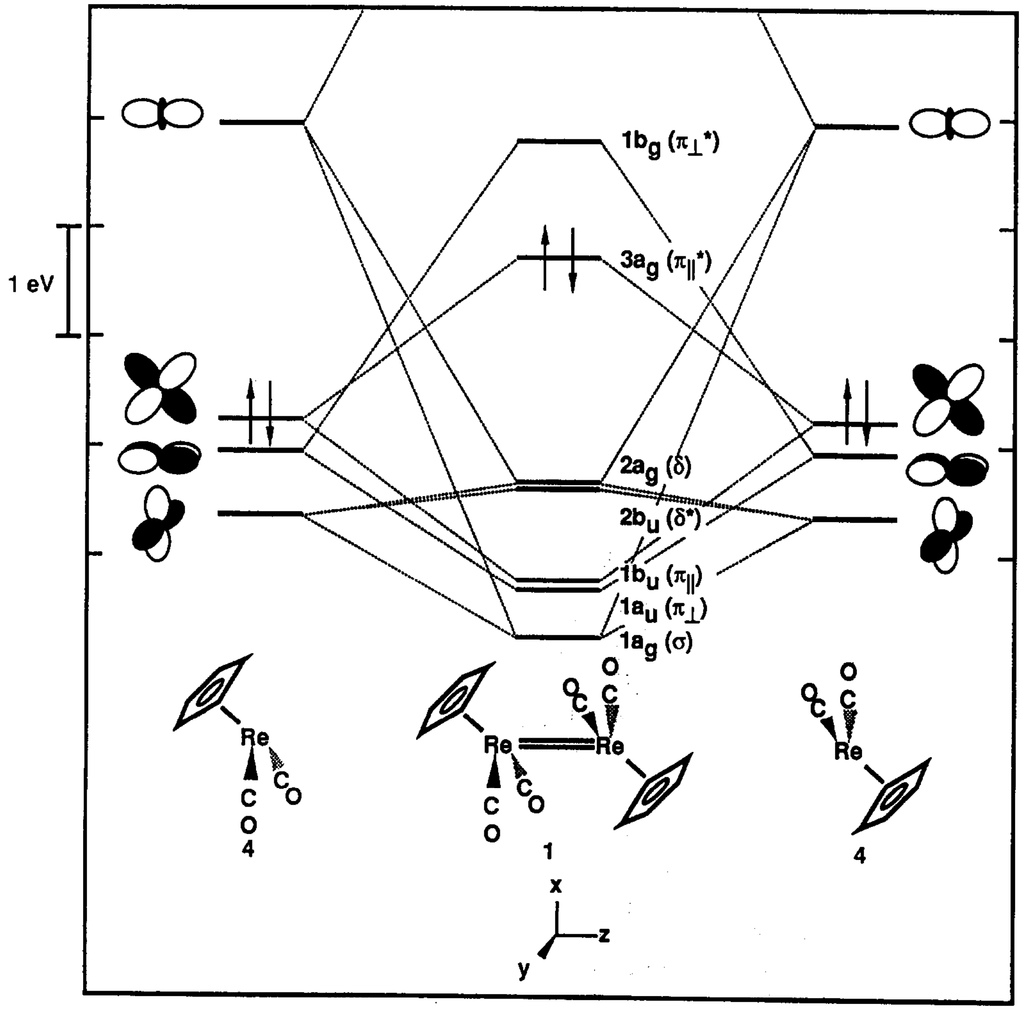

Fig. 2. Molecular orbital diagram for the frontier orbital region of [CpRe(CO)$_2$]$_2$ (**1**). The arrows indicate the highest occupied MO.

action with the OH ligands, are labeled σ and $\pi_\perp$ in Fig. 1. Thus, the picture that emerges for **5** is of a two-electron fragment containing a σ and a π orbital available for dimerization. In this sense, **5** is isolobal with a CH_2 fragment.

We see that both fragments **4** and **5** have frontier orbitals of σ and π symmetry with respect to Re–Re bond formation. The final difference in the available d orbitals in these two fragments reflects the formal oxidation states and electron counts for the Re atoms: d^6 Re^I in **4** *vs.* d^2 Re^V in **5**.

2.2. $[CpRe(CO)_2]_2$ (1) and $[(HC)Re(OH)_2]_2$ (2)

We can now combine the frontier orbitals of fragments **4** and **5** in order to explore the metal–metal bonding in the model dimers **1** and **2**. We shall first consider the combination of two low-valent fragments **4** to form the low-valent dimer **1**. The crystal structure of **1*** shows two semibridging carbonyl ligands [3]. However, we shall focus on the Re–Re bonding by first considering an idealized structure for **1** in which all four carbonyl ligands adopt terminal nonbridging positions (Re–C–O = 180°).

As seen in Fig. 1, the Re 5dσ orbital of **4** is considerably higher in energy than the 5dπ and 5dδ orbitals. However, the combination of a relatively short bond length and relatively diffuse 5d orbitals will foster strong interaction between the 5dσ orbitals of two fragments **4**, assuring that the Re–Re σ-bonding MO will be low in energy. With regard to the Re 5dπ orbitals of **4**, the preceding discussion showed that while both 5dπ orbitals are low in energy, they are not degenerate because of their differing orientations relative to the Cp ligand.

Figure 2 shows the MO diagram of the C_{2h} model complex **1**, obtained by interaction of the orbitals of two fragments **4** in a transoid orientation. The lowest three Re–Re MOs of **1** ($1a_g$, $1a_u$ and $1b_u$) represent the formation of one Re–Re σ and two Re–Re π bonds, although there is significant mixing of the Re 5dδ orbital in the $1a_g$ MO. It is notable that the Re–Re σ-bonding MO is much lower in energy than the corresponding orbital of $[CpMn(CO)_2]_2$ in an earlier calculation by Lichtenberger *et al.* [10] In this calculation (which was an intermediate calculation in an analysis of the bonding in $[CpMn(CO)_2]_2(\mu\text{-}CH_2)$), the longer bond length and more contracted Mn 3d orbitals led to a σ-bonding MO of significantly higher energy. The $2b_u$ and $2a_g$ MOs of **1** represent the nonbonding δ and δ^* interactions between the two fragments; these MOs have no bearing on the Re–Re bonding in **1**. The final two MOs in Fig. 2 are two π^* orbitals of a_g and b_g symmetry. The occupied $3a_g$ MO is roughly 1 eV lower in energy than the empty $1b_g$ MO, an observation that will be discussed below. Thus, the electron configuration of **1** is $\sigma^2\pi_\perp^2\pi_\parallel^2\delta^2\delta^{*2}\pi_\parallel^{*2}$, corresponding to a diamagnetic complex with a net Re–Re double bond. The electronic structure of **1** can be compared with that for the related d^5–d^5 complexes $Cp_2M_2(CO)_4$ (M = Cr, Mo, W), which have electron configurations of $\sigma^2\pi_\perp^2\pi_\parallel^2\delta^2\delta^{*2}$ and metal–metal triple bonds [16,17].

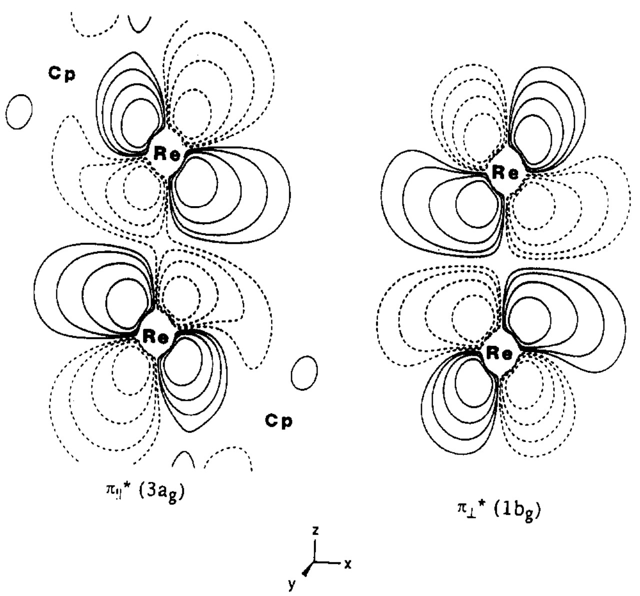

Fig. 3. Contour plots of the Re–Re π^* MOs of **1**. Contour values are ±0.1, ±0.05, ±0.025 and ±0.0125.

The diamagnetic electronic structure of **1** can be contrasted with the situation in higher symmetry d^6–d^6 dimers, such as $Ru_2(O_2CR)_4$ (**8**) [18]. The D_{4h} symmetry of **8** demands two-fold degeneracy of both the Ru–Ru π and π^* MOs. The electron configuration of **8** is $\sigma^2\pi^4\delta^2\delta^{*2}\pi^{*2}$, which also corresponds to a metal–metal double bond. However, because the π^* MOs of **8** are doubly degenerate, **8** possesses a triplet ground state.

The inequivalence and nondegeneracy of the Re–Re π^* MOs of **1** are a consequence of the relative orientations of the $\pi_\perp$ and $\pi_\parallel$ frontier orbitals of fragment **4**. Although the π-bonding MOs ($1a_u$ and $1b_u$) formed from these orbitals are fairly close in energy, the $\pi_\parallel^*$ MO ($3a_g$) is significantly lower than the $\pi_\perp^*$ MO ($1b_g$). A symmetry-based explanation for the lower energy of the $\pi_\parallel^*$ is evident in the contour plots of the two π^* orbitals (Fig. 3). It is evident from this figure that the $\pi_\parallel^*$ MO is slightly less antibonding than the $\pi_\perp^*$ MO. This effect originates in the symmetry requirements of the fragment orbitals. For each fragment **4**, the two lobes of the $\pi_\perp$ orbital are related by the mirror plane of symmetry; as such, these fragment orbitals are ‘forced’ into an orientation that leads to optimum antibonding (see below). In contrast, the lobes of the $\pi_{\parallel}$ orbital of fragment **4** lie in the symmetry plane of the fragment, and can thus be rotated within the plane. Indeed, the $\pi_{\parallel}$ fragment orbitals are seen to 'tip away' from the Cp, through small but significant admixture of Re 5dδ and 5dσ character. The resulting $\pi^*_{\parallel}$ MO, shown below, is thus less antibonding than the $\pi^*_{\perp}$ MO; in essence, the antibonding in the $\pi^*_{\parallel}$ MO has been decreased by mixing in a small amount of Re–Re δ and σ bonding. The $\pi^*_{\parallel}$ MO is therefore at a lower energy than the $\pi^*_{\perp}$ MO, which has no analogous source of stabilization.

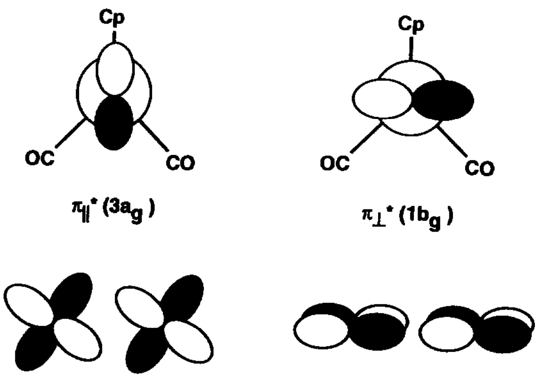

The gap between the two π^* MOs of **1** is further magnified when the idealized structure with terminal carbonyls is changed to the actual geometry of **1**. The structure of **1*** shows two semibridging COs, with Re–C–O angles of 165° and Re–C distances of 1.92 Å and 2.49 Å [3]. These two semibridging carbonyls lie in the same plane as $\pi^*_{\perp}$. As a result, when the carbonyls are moved into semibridging positions, they interact preferentially with the $\pi^*_{\perp}$ MO of **1**, further destabilizing that unoccupied orbital while preserving the Re–Re double bond [19]. Thus, the effect of allowing the carbonyls to adopt the experimental geometry is to

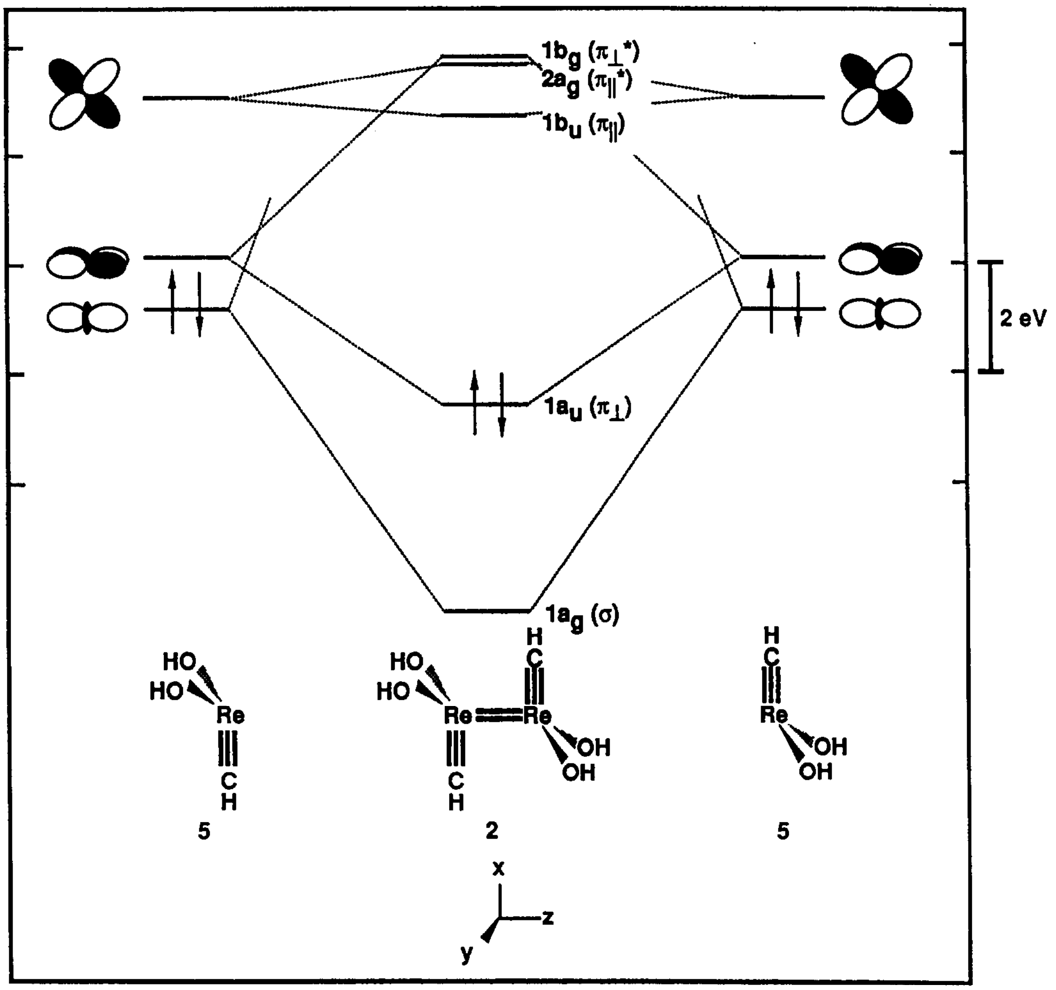

Fig. 4. Molecular orbital diagram for the frontier orbital region of $[HCRe(OH)_2]_2$ (**2**). The arrows indicate the highest occupied MO.

enlarge the HOMO–LUMO gap and to provide a more compelling reason for the molecule to prefer a diamagnetic singlet ground state.

We will now turn to the d^2–d^2 dimer **2**. Although the double bond in **2** appears somewhat more unusual than the one in **1**, its electronic description is considerably simpler. The combination of two fragments **5** to form **2** in a C_{2h} geometry is depicted in Fig. 4. The low-lying σ and π frontier orbitals of **5** combine in a straightforward fashion to produce σ ($1a_g$) and π ($1a_u$) MOs as the lowest orbitals in the Re–Re bonding manifold. These two orbitals are fully occupied, leading to a $\sigma^2\pi^2$ Re–Re double bond and a diamagnetic compound. We pointed out earlier that **5** is isolobal with CH_2. Consistent with this notion, the Re–Re bonding in **2** is similar to that in ethylene. Note that the Re–Re π bond in **2** lies in the plane normal to the C–Re–Re–C plane. The few other compounds that contain d^2–d^2 double bonds, *i.e.* $[Mo(OR)_2(NMe_2)(\mu\text{-}NMe_2)]_2$ [20], $[WCl_2(OR)(ROH)(\mu\text{-}OR)]_2$ [21] and $[CpM(\mu\text{-}X)_2]_2$ (M = Ta, X = Br; M = Nb, X = Cl) [22,23], all contain bridging ligands that will interact with the Re–Re π bond (and, to a lesser extent, the σ bond). Thus, the description of the double bond in **2** is much less complicated than that in these other molecules.

The structure of **2′** indicates a nearly planar transoid C≡Re=Re≡C linkage. Although the steric bulk of the ^{t}Bu ligands will favor a *trans* arrangement of the two Re≡CR fragments, the planar arrangment is also preferred electronically. In Fig. 1 it was seen that the π frontier orbitals of **5** are energetically separated to a greater extent than those in **4**. In order that the lower energy $\pi_\perp$ orbital on each fragment **5** should be capable of interacting in an optimal manner with the other, a planar C≡Re=Re≡C structure must be adopted. If the dihedral angle between the two C–Re–Re planes is 90°, the $\pi_\perp$ orbital on one **5** is forced to interact preferentially with the high energy $\pi_\parallel$ orbital on the other fragment **5**, a less favorable situation. We find that upon rotation about the Re–Re bond, the HOMO–LUMO gap shrinks from a value of 4.5 eV for the *trans* structure to 0.2 eV for the structure with a 90° dihedral angle. We therefore expect an electronic barrier to rotation about the Re–Re bond, independent of any substituent effects.

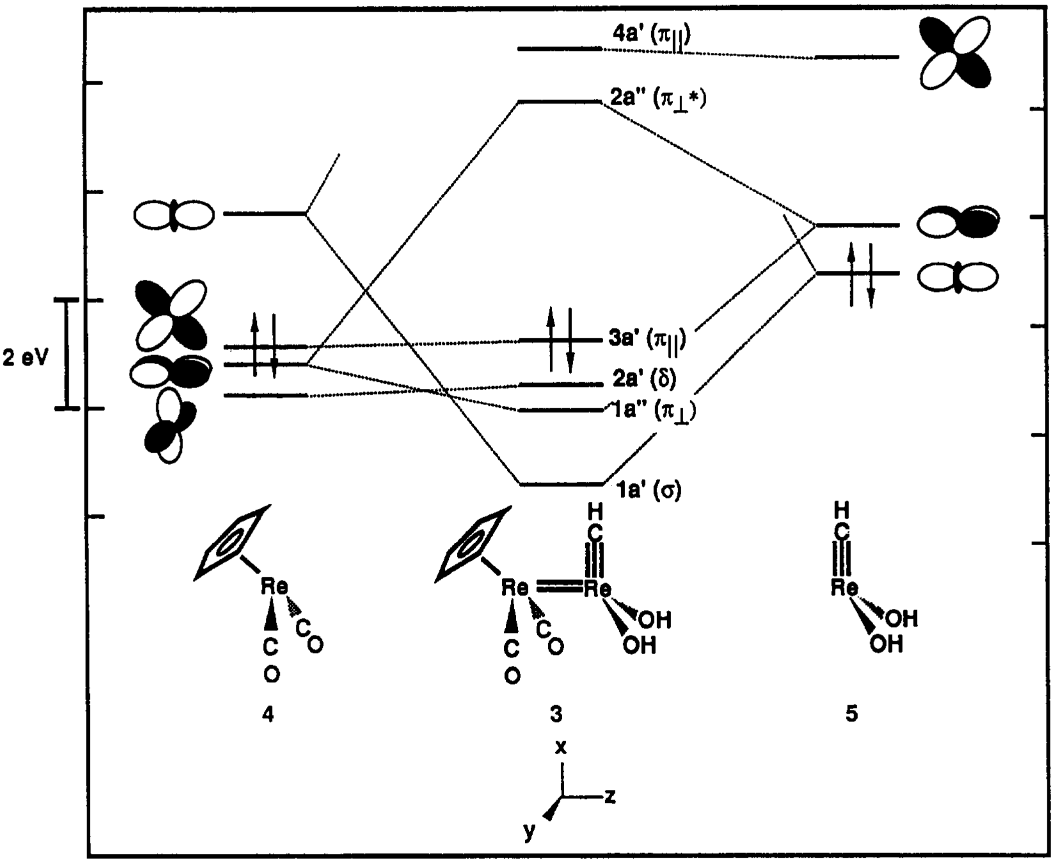

Fig. 5. Molecular orbital diagram for the frontier orbital region of $[CpRe(CO)_2][Re(CH)(OH)_2]$(**3**). The arrows indicate the highest occupied MO.

Both **1** and **2** are seen to have electronic structures consistent with the presence of Re–Re double bonds. The electron distributions in **1** and **2** reflect the difference in the formal oxidation state of Re in the two compounds: the total Re 5d population per Re atom is 5.53 in **1** and 4.59 in **2**. The lower formal oxidation state (and hence larger effective radius) of Re in **1** relative to **2** is particularly manifested in the Re–Re bond lengths of the compounds, 2.723 Å in **1*** [3] *vs.* 2.396 Å in **2′** [4]. The fact that these two systems both possess Re–Re double bonds, but that the bond lengths differ by more than 0.3 Å, provides another example of why caution must be exercised in the correlation of bond length with bond order [24].

2.3. *[CpRe(CO)$_2$][HCRe(OH)$_2$] (3)*

The discussion of the 'homonuclear' dirhenium complexes formed from fragments **4** and **5** leads to the interesting question of whether a 'heterodinuclear' Re–Re dimer **3** could be made by combining one fragment **4** with one fragment **5**. Although compound **3** is not yet known, it is not unreasonable to consider whether the combination of a low-valent Re^I fragment with a high-valent Re^V fragment can lead to Re–Re bond formation. Several mixed-valent compounds have been isolated and fully characterized, such as the d^3–d^5 Re^{IV}–Re^{II} dimer (RO)$_2$Cl$_2$ReReCl$_2$(PPh$_3$)$_2$ [25,26] and the d^2–d^4 Mo^{IV}–Mo^0 complex (^{i}PrO)$_4$MoMo(dmpe)$_2$ [27]. We have examined the electronic structure of this latter compound and found that the metal–metal bonds are polarized due to the asymmetric charge distribution [7].

The results presented here are based on a C_s geometry for **3** in which the Cp–Re bond of **4** and the HC–Re bond of **5** are eclipsed:

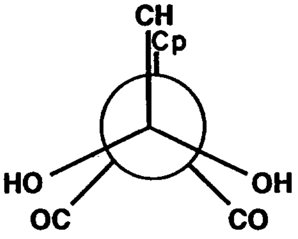

In this geometry, the $\pi_\perp$ orbitals of the two fragments (Fig. 5) are oriented to allow interaction with one another. Because the π orbitals of **4** are close in energy, other rotamers of **3** lead to similar results and are not discussed here. The σ orbitals of **4** and **5** combine to form the 1a′ Re–Re σ-bonding MO of **3**. Likewise, the two $\pi_\perp$ orbitals combine to form the 1a″ Re–Re π-bonding MO. These two MOs are occupied. The remaining four electrons of this d^6–d^2 complex reside in the 2a′ and 3a′ MOs of **3**, which are localized on the low-valent fragment **4**.

The relative polarity of the Re–Re σ- and π-bonding MOs can be estimated by examining the energies of the interacting orbitals, and by using Mulliken population analysis [28]. In the formation of the 1a′ bonding MO, the dσ orbitals from **4** and **5** are at nearly the same energy. The 1a′ MO should therefore be composed of nearly equal contributions from these two fragment orbitals. Consistent with this notion, population analysis of the 1a′ MO indicates that it contains 27% **4** dσ and 34% **5** dσ, as well as a significant admixture of the dδ orbital of **4**. The situation is very different for the Re–Re π-bonding (1a″) and π^*-antibonding (2a″) MOs. The $\pi_\perp$ orbital of the low-valent fragment **4** is considerably lower in energy than that of **5**, which leads to polarization of the 1a″ MO toward the Re^I center. The 1a″ MO contains 65% **4** d$\pi_\perp$ and 30% **5** d$\pi_\perp$. Correspondingly, the 2a″ MO contains 30% **4** and 67% **5**. The polarization of the 1a″ orbital toward the low-valent fragment is reminiscent of that found in calculations for early–late heterobimetallic complexes [29]. Overall, based on the comparative total Re 5d populations, approximately 0.20 e is transferred from fragment **5** to fragment **4** during the formation of **3**.

The above analysis would seem to indicate that, on electronic grounds, there is no reason to preclude the formation of a mixed high-valent/low-valent Re–Re bonded complex such as **3**. Of course, attempts to synthesize compounds such as **3** are expected to lead to some complications beyond this simplified analysis. For example, the Re^V center of **5** is expected to be fairly oxophilic, and there might be significant interactions between the oxygen atoms of the carbonyl ligands and this center. Nevertheless, we hope that these studies will encourage the exploration of new dirhenium complexes based on the combination of d^2 and d^6 moieties.

3. Computational details

The molecular orbital calculations were performed using the Fenske–Hall approximate MO method [30]. The atomic positions for the model complexes **1** and **2** were taken from the crystal structures for [Cp*Re(CO)$_2$]$_2$ [3] and [Re(C^{t}Bu)(O^{t}Bu)$_2$]$_2$ [4], respectively, and idealized to C_{2h} symmetry in each case. Calculations on **1** were performed in the observed geometry, with semibridging carbonyls, and in an idealized geometry in which all carbonyl ligands were terminal with Re–C–O = 180°. The structure of each fragment of **3** was that used for the fragment in the parent dimer; the assumed Re–Re distance (2.56 Å) was the average of the Re–Re distances in **1** (2.723 Å) and **2** (2.396 Å). For **1** and **3**, the cyclopentadienyl rings were constrained to local D_{5h} symmetry, with a C–H distance of 1.05 Å. In **2** and **3**, the alkylidyne C–H and hydroxide

O–H distances were 1.05 Å and 0.98 Å, respectively. Calculations of **3** were performed for three rotamers corresponding to a Cp(centroid)–Re–Re–C(alkylidyne) dihedral angle of 0°, 90° and 180°. The results were not strongly dependent on the choice of dihedral angle and only the results for the dihedral angle set to 0° are presented here.

The atomic wavefunctions were generated by the method of Bursten, Jensen and Fenske [31]. Contracted double-ζ representations were used for the Re 5d AOs and for the C and O 2p AOs. An exponent of 1.16 was used for the hydrogen 1s AO. The basis functions for **1** and the low-valent portion of **3** were derived from the Re(+1), C(0) and O(0) oxidation states. The basis functions for **2** and the high-valent portion of **3** were derived from the Re(+2), C(−0.5) and O(−0.5) oxidation states. In both cases the Re 6s and 6p exponents were fixed at 2.0. The CO 3σ orbitals and the first three occupied C_5H_5 orbitals were filled with 2.0 electrons and deleted from the basis transformation set in all calculations [32]. The CO 6σ orbitals and the virtual orbitals of C_5H_5 above the e_2'' level (D_{5h}) were filled with 0.0 electrons and deleted from the basis transformation set in all calculations [32].

The calculations were performed using a fragment approach. For all three compounds, the ligands were converged as independent fragments, the resulting molecular orbitals of which were then allowed to interact with the two rhenium atoms. The CO ligand was converged as a neutral molecule, the OH and Cp ligands were converged as anions and the CH ligand as the trianion. All calculations were converged by a self-consistent-field iterative technique using a convergence criterion of 0.001 as the largest deviation of atomic orbital populations between successive cycles.

Acknowledgements

We gratefully acknowledge the support of the National Science Foundation through research grants (B.E.B. and C.P.C.) and a Predoctoral Fellowship (T.A.B.). T.A.B. also thanks the Monsanto Co. for generous financial support from a Summer Research Opportunites for Undergraduates Program. C.P.C. also gratefully acknowledges support from the US Department of Energy, Division of Basic Energy Sciences.

References

1 M.J. Winter, *Adv. Organomet. Chem.*, *29* (1989) 101.
2 F.A. Cotton and R.A. Walton, *Multiple Bonds between Metal Atoms*, Clarendon, Oxford, 1993.
3 (a) C.P. Casey, H. Sakaba, P.N. Hazin and D.R. Powell, *J. Am. Chem. Soc.*, *113* (1991) 8165; (b) C.P. Casey, Y. Ha and D.R. Pavell, *J. Am. Chem. Soc.*, *116* (1994) 3424..
4 R. Toreki, R.R. Schrock and M.G. Vale, *J. Am. Chem. Soc.*, *113* (1991) 3610.
5 (a) J.P. Blaha, B.E. Bursten, J.C. Dewan, R.B. Frankel, C.L. Randolph, B.A. Wilson and M.S. Wrighton, *J. Am. Chem. Soc.*, *107* (1985) 4561; (b) B.E. Bursten and R.H. Cayton, *Organometallics*, *5* (1986) 1051; (c) B.E. Bursten and R.H. Cayton, *J. Am. Chem. Soc.*, *108* (1986) 8241; (d) B.E. Bursten and R.H. Cayton, *J. Am. Chem. Soc.*, *109* (1987) 6053; (e) B.E. Bursten, R.H. Cayton and M.G. Gatter, *Organometallics*, *7* (1988) 1342; (f) B.E. Bursten and R.H. Cayton, *Organometallics*, *7* (1988) 1349; (g) B.E. Bursten and R.H. Cayton, *Polyhedron*, *7* (1988) 943; (h) B.E. Bursten and R.H. Cayton, *Inorg. Chem.*, *28* (1989) 2846; (i) H.B. Abrahamson, G.P. Niccolai, D.M. Heinekey, C.P. Casey and B.E. Bursten, *Angew. Chem.*, *104* (1992) 464; *Angew. Chem., Int. Ed. Engl.*, *31* (1992) 471.
6 B.E. Bursten and R.H. Cayton, *Organometallics*, *6* (1987) 2004.
7 B.E. Bursten and W.F. Schneider, *Inorg. Chem.*, *28* (1989) 3292.
8 P. Hofmann, *Angew. Chem., Int. Ed. Engl.*, *16* (1977) 536.
9 D.C. Calabro and D.L. Lichtenberger, *J. Am. Chem. Soc.*, *103* (1981) 6846.
10 D.C. Calabro, D.L. Lichtenberger and W.A. Herrmann, *J. Am. Chem. Soc.*, *103* (1981) 6852.
11 M. Creswick, I. Bernal and W.A. Herrmann, *J. Organomet. Chem.*, *172* (1979) C39.
12 D.L. Lichtenberger and R.F. Fenske, *J. Am. Chem. Soc.*, *98* (1976) 50.
13 M.H. Chisholm, D.M. Hoffman and J.C. Huffman, *Inorg. Chem.*, *22* (1983) 2903.
14 N.M. Kostic and R.F. Fenske, *J. Am. Chem. Soc.*, *103* (1981) 4677.
15 B.E.R. Schilling and R. Hoffmann, *J. Am. Chem. Soc.*, *101* (1979) 3456.
16 E.D. Jemmis, A.R. Pinhas and R. Hoffmann, *J. Am. Chem. Soc.*, *102* (1980) 2576.
17 B.J. Morris-Sherwood, C.B. Powell and M.B. Hall, *J. Am. Chem. Soc.*, *106* (1984) 5079.
18 F.A. Cotton and M. Matusz, *J. Am. Chem. Soc.*, *110* (1988) 5761.
19 G.P. Niccolai, *Ph.D. Thesis*, University of Wisconsin–Madison, 1992.
20 M.H. Chisholm, C.E. Hammond and J.C. Huffman, *Polyhedron*, *8* (1989) 129.
21 D. DeMarco, T. Nimry and R.A. Walton, *J. Am. Chem. Soc.*, *103* (1980) 5078.
22 P.A. Belmonte, F.G.N. Cloke, K.H. Theopold and R.R. Schrock, *Inorg. Chem.*, *23* (1984) 2365.
23 C. Ting and L. Messerle, *Inorg. Chem.*, *28* (1989) 171.
24 F.A. Cotton, *Chem. Soc. Rev.*, *12* (1983) 35.
25 A.R. Chakravarty, F.A. Cotton, A.R. Cutler and R.A. Walton, *Inorg. Chem.*, *25* (1986) 3619.
26 A.R. Chakravarty, F.A. Cotton, A.R. Cutler, S.M. Tetrick and R.A. Walton, *J. Am. Chem. Soc.*, *107* (1985) 4795.
27 M.H. Chisholm, J.C. Huffman and W.G. Van Der Sluys, *J. Am. Chem. Soc.*, *109* (1987) 2514.
28 R.S. Mulliken, *J. Chem. Phys.*, *23* (1955) 1833.
29 See, for example, B.E. Bursten and K.J. Novo-Gradac, *J. Am. Chem. Soc.*, *109* (1987) 904.
30 M.B. Hall and R.F. Fenske, *Inorg. Chem.*, *11* (1972) 768.
31 B.E. Bursten, J.R. Jensen and R.F. Fenske, *J. Chem. Phys.*, *68* (1978) 3320.
32 D.L. Lichtenberger and R.F. Fenske, *J. Chem. Phys.*, *64* (1976) 4247.